

# Graphene on Single-Crystal Diamond for Electronic Applications: A Brief Review

Aisuloo Aitkulova,\* Saman Majdi, Nattakarn Suntornwipat, and Jan Isberg

Graphene on diamond has emerged as a promising platform for various electronic applications. This brief review article explores the recent advancements and the potential of graphene on diamond for electronic applications with a focus on single-crystal (SC) chemically vapor-deposited and high-pressure and high-temperature diamond. Device fabrication techniques, properties, and performance of single-layer graphene on diamond in various electronic devices are discussed. This hybrid system's challenges and prospects are also analyzed. A particular emphasis is placed on the unique benefits of diamond as a substrate for graphene and its growth, including its high thermal conductivity, mechanical strength, high optical phonon energy, and the importance of achieving high-quality single-layer graphene on SC diamond.

## 1. Introduction

Diamond and graphene, both carbon-based materials, exhibit fundamentally distinct electronic properties due to their different atomic hybridizations. They have been extensively studied separately for their electronic, magnetic, and quantum properties.<sup>[1,2]</sup>

Diamond, with its  $sp^3$  hybridization, is a wide-bandgap insulator ( $\approx 5.5$  eV) known for its room-temperature (RT) high carrier mobilities of electrons and holes,<sup>[3]</sup> high thermal conductivity,<sup>[4,5]</sup> high breakdown field strength, and exceptional mechanical properties.<sup>[6]</sup> On the other hand, graphene features  $sp^2$  hybridization, forming a 2D honeycomb lattice. This structure gives graphene a semimetallic behavior with a zero bandgap and linear energy-momentum dispersion near the Dirac points. As a result, graphene can exhibit an extraordinary carrier mobility of  $10\,000\text{ cm}^2\text{ Vs}^{-1}$  at RT and  $100\,000\text{ cm}^2\text{ Vs}^{-1}$  at 2.3 K.<sup>[7]</sup> In addition, graphene has unique quantum properties, such as massless

charge carriers, and its high thermal conductivity<sup>[8]</sup> and mechanical flexibility make graphene highly versatile.

The significance of combining diamond and graphene lies in the potential to harness the best of both: diamond's insulating and heat-dissipating properties and graphene's outstanding electrical characteristics.


Diamond exhibits a high optical phonon energy of 165 meV.<sup>[9]</sup> This property can be vital for graphene-on-diamond devices, as the carrier mobility in the graphene layer is often limited by optical phonon scattering originating from the substrate. A high optical phonon energy implies that few optical phonons are present at RT, leading to a low scattering rate. Other benefits of diamond as a substrate include that it has a chemically inert surface with low trap density compared with conventional  $\text{SiO}_2/\text{Si}$  and  $\text{SiC}$ . As a substrate for graphene-on-diamond devices, chemical vapor deposition (CVD) diamond is preferable to high pressure high temperature (HPHT) due to its scalability possibility and lower defect density.<sup>[10]</sup> The exceptional properties of graphene and diamond have sparked a growing interest in integrating these materials for electronic and quantum applications.<sup>[11]</sup>

There are numerous applications for diamond and graphene. Diamond-based active components have demonstrated prominent potential in power electronics, such as Schottky diodes, field-effect transistors (FET) (p-type, n-type), light-emitting diode, as well as sensors and photodetectors,<sup>[12–16]</sup> and also known for passive applications and heat sinks.<sup>[5,17]</sup> Correspondingly, graphene-based active devices like diodes and FETs have also shown promise in amplifying power-detecting applications,<sup>[18,19]</sup> optoelectronic synapses,<sup>[20]</sup> as well as heat spreaders for power electronics.<sup>[21]</sup> This hybrid system could revolutionize high-frequency electronics, thermal management, and quantum sensing.<sup>[22,23]</sup>

Thus, understanding the methods to effectively integrate these materials—through approaches like wet transfer or direct growth—is crucial for developing next-generation devices. The first method involves the common wet transfer technique. CVD graphene is synthesized on the initial substrate, usually metal,<sup>[8]</sup> and then transferred to the desired substrate using a sacrificial polymer-based film.<sup>[24]</sup> The second method entails directly growing graphene or graphene-like layer on a diamond using a catalyst in combination with either precursor materials or rapid thermal processing (RTP).<sup>[25,26]</sup>

This review article provides updates on these two methods of depositing graphene film on a diamond surface: the wet transfer method and the direct growth method, while discussing the advantages and limitations of each method, such as the quality

A. Aitkulova, S. Majdi, N. Suntornwipat, J. Isberg  
Division for Electricity  
Department of Electrical Engineering  
Uppsala University  
Box 65, 751 03 Uppsala, Sweden  
E-mail: aisuloo.aitkulova@angstrom.uu.se

 The ORCID identification number(s) for the author(s) of this article can be found under <https://doi.org/10.1002/pssa.202400567>.

© 2024 The Author(s). physica status solidi (a) applications and materials science published by Wiley-VCH GmbH. This is an open access article under the terms of the Creative Commons Attribution-NonCommercial License, which permits use, distribution and reproduction in any medium, provided the original work is properly cited and is not used for commercial purposes.

DOI: 10.1002/pssa.202400567

of graphene obtained, scalability, and compatibility with existing semiconductor fabrication processes.

## 2. Graphene Transfer

Transferring graphene onto diamond is a useful method for fabricating heterostructures. One common approach involves wet transfer using a sacrificial polymer layer deposited on graphene on the growth substrate.<sup>[27]</sup> This is then etched prior to being transferred onto the final substrate, in this case, diamond. Extensive research and optimization of the transfer process for silicon substrates have led to enhanced controllability with this method. However, some challenges need to be addressed when dealing with diamond as the final substrate.

These challenges include the low visibility of graphene on a transparent substrate and the relatively poor adhesion of graphene to diamond, which can be improved by pretreatment methods such as oxygen plasma treatment or functionalization of the diamond surface with chemical groups that enhance the adhesion. Also, graphene can be cleaned during transfer with an optimized Radio Corporation of America (RCA) clean procedure.<sup>[24]</sup> Moreover, the transfer process should also consider the potential impact on the quality and properties of both graphene and diamond.<sup>[11]</sup> Due to the thermal properties of diamond, Yu et al. demonstrated that utilizing diamond as a substrate results in 18 times higher breakdown current flowing through graphene compared to SiO<sub>2</sub>/Si. Moreover, the breakdown current is one order higher on single-crystalline diamond than on the ultrananocrystalline diamond (UNCD).<sup>[28]</sup>

### 2.1. Transfer Conditions

Monitoring the quality evolution of graphene during the wet transfer process is crucial because the process can significantly impact the properties of the final graphene film.<sup>[29]</sup> This process can introduce strain, doping, and defects, affecting graphene.<sup>[29]</sup> Maintaining a high quality of graphene during the transfer process is essential for ensuring optimal device performance. The high optical contrast of graphene on its substrate facilitates the transfer process control and following device fabrication.

The most common methods to identify graphene on substrate (SiO<sub>2</sub>/Si) include optical microscopy and Raman spectroscopy, which are complicated to perform on single-layer graphene on diamond. One of the reasons is the intense first-order Raman peak at around 1332 cm<sup>-1</sup>. The second is the transparency of diamond. Third, interaction between graphene and substrate introduces strain. Together with charged impurities, this results in

G and 2D band shift and broadening.<sup>[30]</sup> For SiO<sub>2</sub>, the most suitable thickness for graphene visibility is 300 nm.<sup>[31]</sup> A slight change in thickness can make graphene invisible by decreasing the optical contrast. In addition, SiO<sub>2</sub>/Si is not a transparent substrate.

In the case of diamond, the situation is more complicated. Articles about single-layer graphene on diamond rarely include optical images of graphene on diamond unless it is stacked or covered with a layer of hexagonal boron nitride (hBN) or metal oxide.<sup>[22]</sup> Using Fresnel's law, finding the most suitable thickness of UNCD diamond with higher optical contrast on top of Si substrate is possible, 0.65 μm for 555 nm wavelength.<sup>[28]</sup> This thickness for SC diamond is not commonly available on the market and is difficult to handle without a supporting substrate.

### 2.2. Substrate Effect on Graphene

#### 2.2.1. Graphene on a Diamond Substrate

Meric and colleagues explored the relationship between saturation velocity and Fermi velocity, represented by the equation

$$v_{\text{sat}} = v_f \left( \frac{E_{\text{phonon}}}{E_F} \right) \quad (1)$$

for graphene field-effect transistors (GFETs) on SiO<sub>2</sub>/Si.<sup>[32]</sup> This suggests that the carrier saturation velocity can be increased utilizing a substrate with higher (optical) phonon energy, such as diamond, with its extremely high optical phonon energy, 165 meV.

This physical property of diamond leads to device improvement by increasing the extrinsic maximum frequency of oscillation of GFETs,  $f_{\text{MAX}}$ , representing the highest frequency at which the transistor can operate as an oscillator before its gain drops below one. On SiO<sub>2</sub>/Si, Bonmann et al. achieved  $f_{\text{MAX}} = 34$  GHz for 0.5 μm-channel GFET by improving the fabrication process.<sup>[33]</sup> By replacing SiO<sub>2</sub>/Si with diamond, Asad et al. reached  $f_{\text{MAX}} = 55$  GHz for a 0.5 μm-channel device.<sup>[23]</sup> Majdi et al. later considered the impurity concentration in diamond, demonstrating that higher carrier mobility can be achieved in graphene on electronic grade diamond than on optical grade, 2750 versus 290 cm<sup>2</sup> Vs<sup>-1</sup> at RT.<sup>[34]</sup> **Table 1** contains literature information regarding graphene-based device performance.

#### 2.2.2. Scattering in Graphene

The most investigated scattering mechanisms for ballistic transport in graphene are caused by charged impurities, surface polar phonons, and electron-phonon scattering. Studies of carrier

**Table 1.** Summary of devices based on transferred single-layer graphene on diamond.

Article	Diamond	Fabricated device	Contact material	Gate, [nm]	Device size	Carrier type	Bias, [V]	Electron mobility [cm <sup>2</sup> Vs <sup>-1</sup> ]	Hole Mobility, [cm <sup>2</sup> Vs <sup>-1</sup> ]
Majdi <sup>[34]</sup>	CVD (100)	Gated Hall bar	Ti/Pd/Au	23 (Al <sub>2</sub> O <sub>3</sub> )	26 × 8 μm	hole	-5-6	1680	2750
Asad <sup>[23]</sup>	CVD (100)	GFET	Ti/Pd/Au	23 (Al <sub>2</sub> O <sub>3</sub> )	0.5-2 μm	hole	1	-	2000 (eff)
Zhao <sup>[64]</sup>	CVD (100)	Hall bar	Ti/Au	-	-	hole	-	-	≈250
Yu <sup>[28]</sup>	CVD UNCD & SCD (100)	GFET	Ti/Au	20 (HfO <sub>2</sub> )	10-60 μm	both	±4	1520	2590

scattering on the macroscale are still ongoing, even in the case of graphene on SiO<sub>2</sub>/Si. So far, substrate materials that were investigated are: SiO<sub>2</sub>, hBN, Si<sub>3</sub>N<sub>4</sub>, hexamethyldisilazane (HMDS), HfO<sub>2</sub>, Al<sub>2</sub>O<sub>3</sub> and tetraethyl orthosilicate, sapphire, silicon, germanium, polyethylene naphthalate (PEN), polyethylene terephthalate (PET), and quartz.<sup>[35]</sup>

A good-quality substrate with a low concentration of impurities and surface preparation help to decrease the detrimental effect of the substrate.<sup>[36]</sup> There are invasive and noninvasive measurement techniques that provide information about scattering in graphene-based devices: carrier transport measurements, Raman spectroscopy, scanning tunneling microscopy (STM), THz spectroscopy, and angle-resolved photoemission spectroscopy. Electron transport measurements on graphene devices can elucidate scattering mechanisms, caused by charged impurities and mechanical strain affecting mobility.<sup>[37]</sup> Raman spectroscopy probes defect density and doping levels.<sup>[38]</sup> STM can directly visualize atomic structure and electronic properties, shedding light on edge effects, contributing to backscattering and intervalley scattering.<sup>[39]</sup> THz spectroscopy measures Drude mobility, which represents the intrinsic carrier movement, less influenced by larger surface defects like wrinkles and, therefore, more suitable on the nanoscale. In contrast, most transport measurements capture field-effect mobility, influenced by larger surface defects like wrinkles or grain boundaries. Since THz measurements average conductivity over the short distance an electron travels during one optical cycle (tens of nanometers), they are less sensitive to these larger imperfections, providing a more accurate representation of the material's inherent properties.<sup>[35,40]</sup> Besides, roughness of the substrate contributes to increased strain of the film or creates wrinkles and edges that could induce scattering. Scattering caused by the substrate leads to reduced carrier mobility, charge transfer, temperature-dependent resistivity, and self-heating.<sup>[41,42]</sup> The high optical phonon energy and the well-polished surface of SC diamond make it an excellent candidate for combining with graphene. Diamond can also be used in current mapping of graphene utilizing nitrogen vacancy centers, which can sense not only static magnetic fields but also fluctuating ones. This may lead to the possibility of measuring charge fluctuations in graphene.<sup>[43]</sup> Besides, the combination of *sp*<sup>2</sup> and *sp*<sup>3</sup> carbon nanomaterials has proven itself in the nanoscale.<sup>[44]</sup>

### 3. Direct Growth of Graphene on Diamond

The direct growth method involves synthesizing graphene directly on the diamond surface using a metal catalyst (Ni, Cu, and Fe) with a RTP technique.<sup>[45–47]</sup> Another way is to use precursor gases, which are similar to the CVD synthesis of graphene itself. This method offers the advantage of directly integrating graphene onto the diamond substrate, eliminating the need for transfer processes. The main disadvantage of the transfer method is a decrease in interface quality between graphene and diamond, introducing more carrier scattering. Ideally, this approach allows for better control over the growth process and can result in high-quality graphene with good adhesion to the diamond surface. In addition, direct growth provides a scalable and efficient method for integrating graphene with diamond substrates, making it suitable for large-scale production.<sup>[48]</sup> Furthermore, this method is compatible

with existing semiconductor fabrication processes, allowing for the seamless integration of graphene–diamond heterostructures into electronic devices.

#### 3.1. The Process of Graphene Growth in RTP

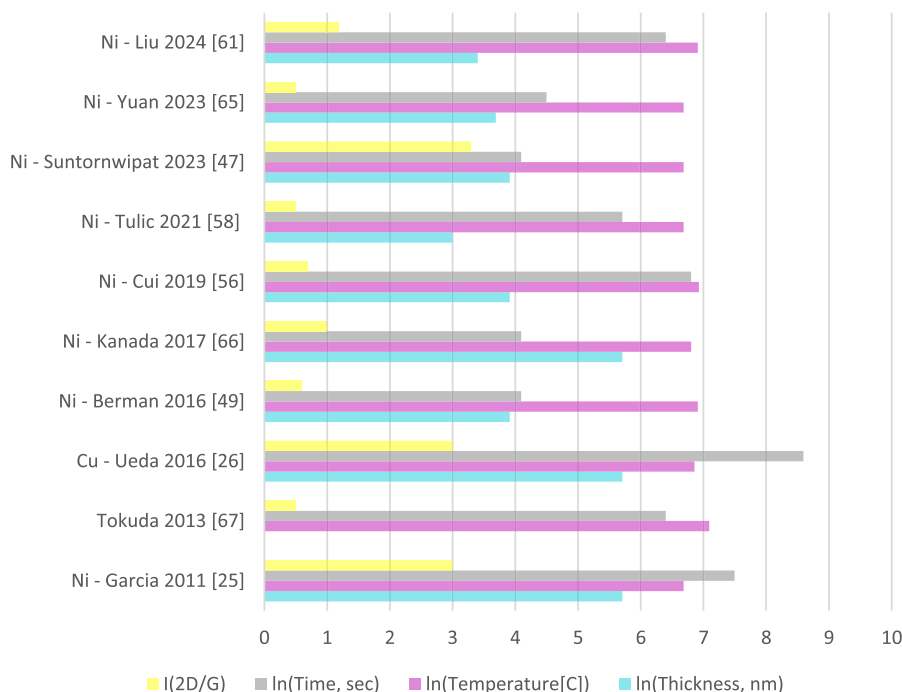
The synthesis of graphene involves at least two processes that can only occur within specific temperature ranges. The latest research on RTP is mainly focused on Ni as a catalyst for graphene/-like growth; the possible reason behind it could be the high carbon solubility and low cost of Ni.<sup>[49]</sup> The first process is the dissolution of carbon in nickel at elevated temperatures, while the second involves “graphene precipitation” on the Ni surface as the carbon atoms crystallize. The activation energy for surface metal is lower than bulk, causing difference in carbon diffusion.<sup>[50]</sup> Diffusion barriers are determined by bulk values, with metal thickness being one of the factors.<sup>[51]</sup> Carbon atoms can move through the lattice or along grain boundaries, requiring varying activation energies.<sup>[52]</sup> It is feasible that the paths for diffusion occur within an imperfect crystal lattice. The distance between the carbon atom and the metal surface layer influences the required activation energy. Additionally, there is a strong connection between nickel thickness and graphene layer quantity that significantly relies on the crystalline nature of the nickel film. Nickel changes during annealing, such as the dewetting process, affecting the resulting uniformity of the graphitized surface. Therefore, even the diffusion path experiences alterations in this process. The growth of graphene on a diamond substrate encompasses several processes, such as carbon dissolving in nickel at elevated temperatures and subsequent precipitation of graphene on the surface of nickel.

#### 3.2. Conditions of Graphene Growth in RTP

**Table 2** chronologically compiles past studies on SC CVD and HPHT diamonds with different orientations, primarily (100) and (111), and nanocrystalline (NCD). Graphitization depends on multiple factors, including the catalyst selection, thickness, and crystallinity of the catalyst, as well as the atmosphere used, heating rate, cooling rate, and duration of heating.<sup>[53]</sup> Most studies are about Ni, but some used Cu and Fe. The atmospheres applied during annealing include Ar, H<sub>2</sub>:Ar, N<sub>2</sub>, H<sub>2</sub>:N<sub>2</sub>, and vacuum. Annealing durations vary from 20 s to 90 min at temperatures between 800 and 1200 °C; in some studies, it varies up to 150 min without distinct conclusions. After annealing, the Ni layer can be etched by sulfuric acid and hydrogen peroxide mixture.<sup>[54]</sup> These studies highlight the complex nature of graphene growth on diamond substrates and the various factors that can influence the process. Some of these articles follow different aims for defining film quality. These aims include characterizing the graphene film's uniformity, number of layers, crystallinity, and coverage on the diamond surface<sup>[55]</sup> (**Figure 1**). Short-time annealing (20s) at 1000 °C and rapid cooling at 500 °C can result in higher uniformity of multilayer graphene.<sup>[54]</sup> So far, improved uniformity of grown film on top of SC diamond compared to UNCD was achieved by doping diamond with boron.<sup>[56]</sup> X-ray photoelectron spectroscopy analysis showed that these films contain more *sp*<sup>3</sup> hybridization than *sp*<sup>2</sup>.

**Table 2.** Growth of graphene/graphite on diamond. Bold details are conditions that lead to more uniformity and a fewer number of graphene-like layers. For roughness column, values in parentheses are AFM scan size.

Article	Diamond	Metal	Thickness [nm]	T [°C]	Atm	Time [s]	Cooling rate [K s <sup>-1</sup> ]	Graphene	Ra [nm]	mobility [cm <sup>2</sup> Vs <sup>-1</sup> ]	Carrier density [cm <sup>-2</sup> ]
Liu <sup>[54]</sup>	HPHT (100)	Ni	30	900–1100	H <sub>2</sub> /Ar 50/ 100 sccm	Up to 60s	–	multi	2.36 nm	737	–
Liu <sup>[63]</sup>	HPHT (100) B-doped	Ni	30	1000	H <sub>2</sub> /Ar 50/ 100 sccm	10 min	–	multi	4 nm (2 μm)	–	–
Yuan <sup>[65]</sup>	CVD/HTPT/EPL	Ni	10–40–100	800	–	1.5 min	–	multi	–	380	1e+11
Suntornwipat <sup>[46]</sup>	CVD (100)	Ni	50–300 nm	800	Ar	1 min	65 K s <sup>-1</sup> heating; 20 K s <sup>-1</sup> cooling	20%	9 nm (20 μm)	Hall 79 at RT, 123 at 80 K	1e+13
Tulic <sup>[57]</sup>	(100) & (111)	Ni	20 nm	800	1e–6 mbar	5 min	–	multi	–	Conductance ≈10 mS at RT	–
Cui <sup>[55]</sup>	(100) HPHT	Ni	50 nm	1020	H <sub>2</sub>	15 min	Naturally	–	–	CV 6.2 Ω cm <sup>-2</sup>	–
Kanada <sup>[66]</sup>	HPHT (111)	Ni	300 nm	900	Ar	1 min	283	–	2 nm (2 μm) 1 l	Hall 140 at RT	5.7e+13
Berman <sup>[48]</sup>	UNCD/Si	Ni	50 nm	800–1000	H <sub>2</sub> /N <sub>2</sub> 5%/95%	1 min	–	monolayer	0.8 nm (5 μm)	FET 20 nm HfO <sub>2</sub> 2e+3 at –0.5 V	3.5e+12
Ueda <sup>[26]</sup>	(111) & (100)	Cu	150–300	950	2 * 10 <sup>-6</sup> Torr	90 min	–	85% monolayer	4 nm (2 μm)	Hall 410 at RT; 670 at 50 K	≈1e+13
Tokuda <sup>[67]</sup>	(111) HPHT	–, H-terminated	–	1000–1300	1–3 Pa	10 min	–	multi	0.1 nm	–	–
Garcia <sup>[25]</sup>	(100) CVD	Ni	30, 80, and 300 nm	800	1e–10–3e–8 mbar	30 min	293 K s <sup>-1</sup> for first 473 K	multi	130 nm (20 μm)	–	–



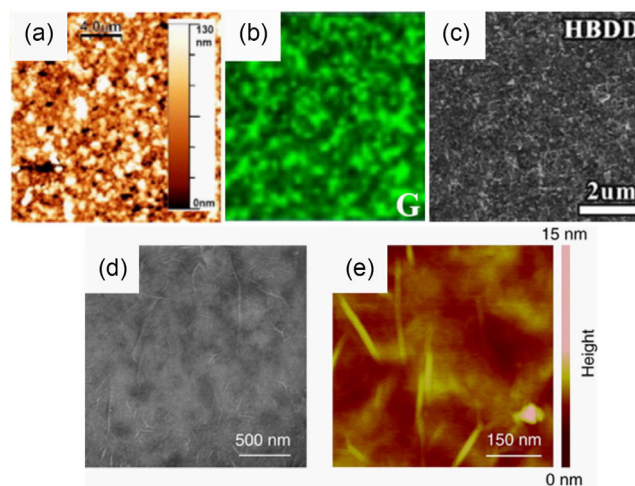
**Figure 1.** Correlation between  $I(2D/G)^{-1}$  ratio and growth parameters: time, temperature, thickness in logarithmic scale.

Figure 1 shows that the current focus of RTP growth is to achieve a uniform monolayer graphene layer by advancing toward lower catalyst thickness and improving temperature control. By removing metal layer, we can decrease number of parameters to control, as well as the dewetting problem, yet process will require higher temperature.

### 3.3. Future Improvements

The Ni dewetting process during annealing is another factor that has not been thoroughly studied. The Ni dewetting process refers to the formation of isolated islands or droplets of nickel on the diamond surface during annealing.<sup>[57]</sup> The dewetting process can be influenced by the properties of the substrate and by the film itself.<sup>[58]</sup> Solid-state dewetting typically takes place at film imperfections and may also be impacted by the structure of the substrate, its morphology, elastic properties, geometry, and grain boundaries in the film. These factors can significantly affect the growth and quality of graphene on diamond substrates and contribute to the variations observed in different studies.<sup>[59]</sup> So far, all works on SC diamond show a strong dewetting effect, resulting in a nonuniform film with different numbers of graphene layers. **Figure 2a** shows an atomic force microscope (AFM) image of the 300 nm-thick Ni film surface on (001) SC diamond with the most substantial dewetting effect. **Figure 2b** shows Raman mapping of the dewetted Cu surface after growth. Introducing boron doping during growth contributes to a smoother surface (**Figure 2c**). The smoothest surface of grown graphene films was achieved with NCD substrate (**Figure 2d,e**).

Leroy et al. concluded that the catalyst thickness and annealing temperature are two main factors in the dewetting kinetics.<sup>[59]</sup>



**Figure 2.** a) AFM image of graphene-like layers on 300 nm Ni after growth. Reprinted with permission.<sup>[25]</sup> Copyright 2011, Elsevier. b) Raman mapping of grown graphene-like layers on Cu after growth. Reprinted with permission.<sup>[26]</sup> Copyright 2016, Elsevier. c) Scanning electron microscope (SEM) image of high boron-doped sample after growth. Reprinted with permission.<sup>[63]</sup> Copyright 2024, Elsevier. d) SEM pictures of grown films on UNCD.<sup>[48]</sup> e) AFM image of grown graphene on UNCD. (d,e) Reused under the terms of the CC BY 4.0 license.<sup>[48]</sup> Copyright 2016, The Authors. Published by Springer Nature.

Other ways of affecting the dewetting kinetics include adding strain or impurities into the substrate, which was also observed in the research of Liu et al. Changing the orientation to (111) did not yield a satisfactory result. Etching in this direction is complex, and the grown film tends to have more defects.<sup>[26,57,60]</sup>

Switching to UNCD and varying thickness can provide better control over the dewetting process and improve the uniformity of the graphene film on diamond substrates.<sup>[60]</sup> Varying partial pressure values for precursor gases, as was shown on CVD-grown graphene, or etching gases during the growth process could improve process control, as they can alter the kinetics of dewetting and promote a more uniform film deposition.<sup>[2,61,62]</sup>

#### 4. Summary

Graphene and diamond are two different allotropes of carbon, and both have been broadly investigated in terms of electrical, quantum, optical, and mechanical properties. Their combination raises many questions. The complex nature of graphene growth on diamond substrates, as highlighted by previous studies, underscores the importance of considering multiple factors such as catalyst selection, thickness, crystallinity, applied atmosphere, heating rate, cooling rate, and duration of heating. Challenges such as reproducible graphene transfer onto a transparent substrate and interface control need to be addressed when transferring graphene onto a diamond.

Future research should focus on the challenges associated with the graphene/diamond interface and further explore the potential of diamond as a substrate for graphene-based electronic devices. The combination of graphene and diamond as fully carbon-based electronic devices represents an exciting frontier in materials science and electronics, and further research and advancements in this area can potentially impact future electronic technology development.

#### Acknowledgements

The authors acknowledge the Swedish Research Council (grant no. 2022-04186) and the Swedish Energy Agency (grant no. P2019-90157) for financial support.

#### Conflict of Interest

The authors declare no conflict of interest.

#### Keywords

chemical vapor deposition, diamonds, electronics, fabrications, graphene, high pressure high temperature, single crystals

Received: July 14, 2024

Revised: December 7, 2024

Published online:

- [1] H. Yang, Y. Ma, Y. Dai, *Funct. Diamond* **2021**, 1, 150.  
 [2] M. Saeed, Y. Alshammari, S. A. Majeed, E. Al-Nasrallah, *Molecules* **2020**, 25, 3856.  
 [3] J. Isberg, J. Hammersberg, E. Johansson, T. Wikström, D. J. Twitchen, A. J. Whitehead, S. E. Coe, G. A. Scarsbrook, *Science* **2002**, 297, 5587.  
 [4] D. J. Twitchen, C. S. J. Pickles, S. E. Coe, R. S. Sussmann, C. E. Hall, *Diamond Relat. Mater.* **2001**, 10, 3.

- [5] C. Zhang, R. D. Vispute, K. Fu, C. Ni, *J. Mater. Sci.* **2023**, 58, 3485.  
 [6] S. E. Coe, R. S. Sussmann, *Diamond Relat. Mater.* **2000**, 9, 1726.  
 [7] W. Guo, M. Zhang, Z. Xue, P. K. Chu, Y. Mei, Z. Tian, Z. Di, *Adv. Mater. Interfaces* **2023**, 10, 2300482.  
 [8] R. Muñoz, C. Gómez-Aleixandre, *Chem. Vap. Deposition* **2013**, 19, 294.  
 [9] A. M. Zaitsev, *Optical Properties of Diamond: A Data Handbook*, Springer, Berlin, NY **2001**.  
 [10] C. E. Nebel, *Funct. Diamond* **2023**, 3, 2201592.  
 [11] W. Hu, Z. Li, J. Yang, *J. Chem. Phys.* **2013**, 138, 5.  
 [12] T. Shimaoka, M. Liao, S. Koizumi, *IEEE Electron Device Lett.* **2022**, 43, 4.  
 [13] A. Lohrmann, S. Pezzagna, I. Dobrinets, P. Spinicelli, V. Jacques, J.-F. Roch, J. Meijer, A. M. Zaitsev, *Appl. Phys. Lett.* **2011**, 251106, 99.  
 [14] V. Jha, H. Surdi, M. F. Ahmad, F. Koeck, R. J. Nemanich, S. Goodnick, T. J. Thornton, *Solid-State Electron.* **2021**, 186, 108154.  
 [15] M. Liao, *Funct. Diamond* **2021**, 1, 29.  
 [16] H. Fei, D. Sang, L. Zou, S. Ge, Y. Yao, J. Fan, C. Wang, Q. Wang, *Front. Phys.* **2023**, 11, 1226374.  
 [17] X. Hao, B. Liu, Y. Li, J. Zhao, S. Zhang, D. Wen, K. Liu, B. Dai, J. Han, J. Zhu, *Diamond Relat. Mater.* **2023**, 135, 109858.  
 [18] M. Saeed, P. Palacios, M. D. Wei, E. Baskent, C. Y. Fan, B. Uzlu, K. T. Wang, A. Hemmetter, Z. Wang, D. Neumaier, M. C. Lemme, *Adv. Mater.* **2022**, 34, 48.  
 [19] Y. Wu, K. A. Jenkins, A. Valdes-Garcia, D. B. Farmer, Y. Zhu, A. A. Bol, C. Dimitrakopoulos, W. Zhu, F. Xia, P. Avouris, Y. M. Lin, *Nano Lett.* **2012**, 12, 6.  
 [20] Y. Mizuno, Y. Ito, K. Ueda, *Carbon* **2021**, 182, 669.  
 [21] Z. Yan, G. Liu, J. M. Khan, A. A. Balandin, *Nat. Commun.* **2012**, 3, 827.  
 [22] C. Zhong, Y. Wang, D. Mai, C. Ye, X. Li, H. Wang, R. Dai, R. Z. Wang, X. Sun, Z. Zhang, *Nano Lett.* **2024**, 16, 4993.  
 [23] M. Asad, S. Majdi, A. Vorobiev, K. Jeppson, J. Isberg, J. Stake, *IEEE Electron Device Lett.* **2022**, 43, 1226374.  
 [24] X. Liang, B. A. Sperling, I. Calizo, G. Cheng, C. A. Hacker, Q. Zhang, Y. Obeng, K. Yan, H. Peng, Q. Li, X. Zhu, H. Yuan, A. R. Hight Walker, Z. Liu, L. Peng, C. A. Richter, *ACS Nano* **2011**, 5, 11.  
 [25] J. M. Garcia, R. He, M. P. Jiang, P. Kim, L. N. Pfeiffer, A. Pinczuk, *Carbon* **2010**, 49, 1006.  
 [26] K. Ueda, S. Aichi, H. Asano, *Diamond Relat. Mater.* **2016**, 63, 148.  
 [27] S. Ullah, X. Yang, H. Q. Ta, M. Hasan, A. Bachmatiuk, K. Tokarska, B. Trzebicka, L. Fu, M. H. Rummeli, *Nano Res.* **2021**, 14, 11.  
 [28] J. Yu, G. Liu, A. V. Sumant, V. Goyal, A. A. Balandin, *Nano Lett.* **2012**, 12, 3.  
 [29] Z. Wu, X. Zhang, A. Das, J. Liu, *RSC Adv.* **2019**, 9, 41447.  
 [30] A. C. Ferrari, D. M. Basko, *Nat. Nano* **2013**, 8, 235.  
 [31] P. Blake, E. W. Hill, A. H. Castro Neto, K. S. Novoselov, D. Jiang, R. Yang, T. J. Booth, A. K. Geim, *Appl. Phys. Lett.* **2007**, 91, 063124.  
 [32] I. Meric, M. Y. Han, A. F. Young, B. Ozyilmaz, P. Kim, K. L. Shepard, *Nat. Nanotechnol.* **2008**, 3, 11.  
 [33] M. Bonmann, M. Asad, X. Yang, A. Generalov, A. Vorobiev, L. Banszerus, C. Stampfer, M. Otto, D. Neumaier, J. Stake, *IEEE Electron Device Lett.* **2019**, 40, 1.  
 [34] S. Majdi, V. Djurberg, M. Asad, A. Aitkulova, N. Suntornwipat, J. Satke, J. Isberg, *Appl. Phys. Lett.* **2023**, 123, 012102.  
 [35] S. Scarfe, W. Cui, A. Luican-Mayer, J. Ménard, *Sci. Rep.* **2021**, 11, 8729.  
 [36] J. H. Gosling, O. Makarovskiy, F. Wang, N. D. Cottam, M. T. Greenaway, A. Patane, R. D. Wildman, C. J. Tuck, L. Turyanska, T. M. Fromhold, *Commun. Phys.* **2021**, 4, 30.  
 [37] K. I. Bolotin, K. J. Sikes, Z. Jiang, M. Klima, G. Fudenberg, J. Honec, P. Kima, H. L. Stormer, *Solid State Commun.* **2008**, 146, 351.  
 [38] A. Eckmann, A. Felten, A. Mishchenko, L. Britnell, R. Krupke, K. S. Novoselov, C. Casiraghi, *Nano Lett.* **2012**, 12, 3925.  
 [39] J. C. Koepke, J. D. Wood, D. Estrada, Z. Ong, K. T. He, E. Pop, J. W. Lyding, *ACS Nano* **2012**, 7, 75.

- [40] A. Tomadin, S. M. Hornett, H. I. Wang, E. M. Alexeev, A. Candini, C. Coletti, D. Turchinovich, M. Kläui, M. Bonn, F. H. L. Koppens, E. Hendry, M. Polini, K. Tielrooij, *Sci. Adv.* **2018**, *4*, 5.
- [41] R. Rengel, J. M. Iglesias, E. Pascual, M. J. Martín, *J. Phys. Conf. Ser.* **2015**, *647*, 012046.
- [42] R. Rengel, E. Pascual, M. J. Martín, *Appl. Phys. Lett.* **2014**, *104*, 23.
- [43] J.-P. Tetienne, N. Dontschuk, D. A. Broadway, A. Stacey, D. A. Simpson, L. C. L. Hollenberg, *Sci. Adv.* **2017**, *3*, 4.
- [44] J. Vejpravová, *Nanomaterials* **2021**, *11*, 2469.
- [45] Y. L. Q. Yuan, Y. Liu, C. Ye, H. Sun, D. Dai, Q. Wei, G. Lai, T. Wu, A. Yu, L. Fu, K. W. A. Chee, C. Lin, *Biosens. Bioelectron.* **2018**, *111*, 117.
- [46] N. Suntornwipat, A. Aitkulova, V. Djurberg, S. Majdi, *Thin Solid Film* **2023**, *770*, 139766.
- [47] S. P. Cooil, F. Song, G. T. Williams, O. R. Roberts, D. P. Langstaff, B. Jørgensen, K. Høydalsvik, D. W. Breiby, E. Wahlström, D. A. Evans, J. W. Wells, *Carbon* **2012**, *50*.
- [48] D. Berman, S. A. Deshmukh, B. Narayanan, S. K. R. S. Sankaranarayanan, Z. Yan, A. A. Balandin, A. Zinovev, D. Rosenmann, A. V. Sumant, *Nat. Commun.* **2016**, *7*, 12099.
- [49] Y. Bleu, F. Bourquard, T. Tite, A. Loir, C. Maddi, C. Donnet, F. Garrelie, *Front. Chem.* **2018**, *6*, 572.
- [50] F. Cinquini, F. Delbecq, P. Sautet, *Phys. Chem. Chem. Phys.* **2009**, *11*, 48.
- [51] A. Wiltner, Ch Linsmeier, T. Jacob, *J. Chem. Phys.* **2008**, *129*, 8.
- [52] B. S. Berry, *J. Appl. Phys.* **1973**, *44*, 8.
- [53] L. Baraton, Z. B. He, C. S. Lee, C. S. Cojocar, M. Châtelet, J.-L. Maurice, Y. H. Lee, D. Pribat, *EPL Europhys. Lett.* **2011**, *96*, 4.
- [54] Y. Liu, T. Wang, L. Wan, Shaoheng Cheng, L. Li, H. Li, *Appl. Surf. Sci.* **2024**, *660*, 660160008.
- [55] N. Cui, P. Guo, Q. Yuan, C. Ye, M. Yang, M. Yang, K. W. A. Chee, F. Wang, L. Fu, Q. Wei, C.-T. Lin, J. Gao, *Sensors* **2019**, *19*, 13.
- [56] M. Rycewicz, A. Nosek, D. H. Shin, M. Ficek, J. G. Buijnsters, R. Bogdanowicz, *Diamond Relat. Mater.* **2022**, *128*, 109225.
- [57] S. Tulić, T. Waitz, M. Caplovicova, G. Habler, V. Vretenar, T. Susi, V. Skakalova, *Carbon* **2021**, *185*, 300.
- [58] Y. Bleu, F. Bourquard, J.-Y. Michalon, Y. Lefkir, S. Reynaud, A.-S. Loir, V. Barnier, F. Garrelie, C. Donnet, *Appl. Surf. Sci.* **2021**, *555*, 149492.
- [59] F. Leroy, Ł. Borowik, F. Cheynis, Y. Almadori, S. Curiotto, M. Trautmann, J. C. Barbé, P. Müller, *Surf. Sci. Rep.* **2016**, *71*, 2.
- [60] M. Nagai, K. Nakanishi, H. Takahashi, H. Kato, T. Makino, S. Yamasaki, T. Matsumoto, T. Inokuma, N. Tokuda, *Sci. Rep.* **2018**, *8*, 6687.
- [61] I. Sharma, G. S. Papanai, S. J. Paul, B. K. Gupta, *ACS Omega* **2020**, *5*, 22109.
- [62] L. Croin, E. Vittone, G. Amato, *Thin Solid Films* **2014**, *573*, 122.
- [63] Y. Liu, X. Zhang, X. Zhai, N. Gao, S. Cheng, L. Li, H. Li, *Diamond Relat. Mater.* **2024**, *141*, 110697.
- [64] F. Zhao, T. T. Nguyen, M. Golsharifi, S. Amakubo, K. P. Loh, R. B. Jackman, *J. Appl. Phys.* **2013**, *114*, 053709.
- [65] X. Yuan, J. Liu, J. Liu, J. Wei, L. Chen, C. Li, *Sci. Talks* **2023**, *8*, 100277.
- [66] S. Kanada, M. Nagai, S. Ito, T. Matsumoto, M. Ogura, D. Takeuchi, S. Yamasaki, T. Inokuma, N. Tokuda, *Diamond Relat. Mater.* **2017**, *75*, 105.
- [67] N. Tokuda, M. Fukui, T. Makino, D. Takeuchi, S. Yamasaki, T. Inokuma, *Jpn. J. Appl. Phys.* **2013**, *52*, 110121.



**Aisuloo Aitkulova** is a Ph.D. student at the Department of Electrical Engineering at Uppsala University. She received a master of science in photonics and quantum materials from the Skolkovo Institute of Science and Technology, where she worked on the development of the dry transfer of graphene for electronics. Her current research interests are the integration and characterization of 2D materials and wide-bandgap semiconductors for electronics, with a focus on graphene and diamond.



**Saman Majdi** is currently working as a senior researcher at the Div. of Electricity in the Diamond Electronics Group, Uppsala University. He received his M.S. (2006) in material physics from the Royal Institute of Technology (KTH) in Stockholm, Sweden. In 2012, he received his Ph.D. entitled “Experimental studies of charge transport in diamond devices,” mainly concerning electrical characterization and charge transport investigation of single-crystal CVD diamond as a collaboration between the UK-based Element Six Ltd. and Uppsala University. He joined the National Institute of Advanced Industrial Science and Technology (AIST) Osaka, Japan (2013), as postdoc. where he conducted work on the growth and characterization of HFCVD diamond. He held an additional postdoc. at Uppsala University (2015). Since 2017 he has been involved in fundamental physics studies as well as preparation and analysis of diamond substrates involving diverse process techniques. In 2020, he received the Docent title with a focus on ultrawide-bandgap materials at Uppsala University.



**Nattakarn Suntornwipat** earned her M.Sc. in material physics and nanotechnology from Linköping University, Sweden, in 2010, and her Ph.D. in engineering science with a specialization in the science of electricity from Uppsala University, Sweden, in 2018. She is currently an assistant professor at Uppsala University. Her research focuses on wide-bandgap semiconductors, particularly single-crystal diamond, and 2D materials such as graphene. She is also actively involved in research on electric vehicles and electromobility.



**Jan Isberg** was born in Stockholm, Sweden, in 1964. He received the M.Sc. in physics in 1987 and the Ph.D. in physics in 1992 from Stockholm University. He then held a postdoc position at the Department of Mathematics at King's College in London during 1993–1994. In 1995, Dr. Isberg joined ABB Corporate Research in Västerås, Sweden, where he did research on power device technology, in particular research on wide-bandgap semiconductors. He is since 2011 employed as professor in electricity at Uppsala University and heads the Diamond Electronics Group at the Department of Electrical Engineering.